β-delayed particle decay of ^{17}Ne into $p+\alpha+^{12}$C through the isobaric analog state in ^{17}F

J. C. Chow,[1,*] J. D. King,[1] N. P. T. Bateman,[1,2,3,†] R. N. Boyd,[4] L. Buchmann,[2] J. M. D'Auria,[3] T. Davinson,[5] M. Dombsky,[2] E. Gete,[2] U. Giesen,[2,3,‡] C. Iliadis,[1,2,§] K. P. Jackson,[2] A. C. Morton,[1,‖] J. Powell,[6] and A. Shotter[5,¶]

[1]*Physics Department, University of Toronto, Toronto, Ontario, Canada M5S 1A7*

[2]*TRIUMF, 4004 Wesbrook Mall, Vancouver, British Columbia, Canada V6T 2A3*

[3]*Department of Chemistry, Simon Fraser University, Burnaby, British Columbia, Canada V5A 1S6*

[4]*Departments of Physics and Astronomy, Ohio State University, Columbus, Ohio 43210*

[5]*Department of Physics and Astronomy, University of Edinburgh, Edinburgh EH9 3JZ, United Kingdom*

[6]*Nuclear Science Division, Lawrence Berkeley National Laboratory, Berkeley, California 94720*

(Received 13 June 2002; published 18 December 2002)

We have observed the breakup of the isobaric analog state at 11.193 MeV in ^{17}F into three particles via three channels: proton decay to the α-unbound 9.585 MeV state in ^{16}O; and α decay to the proton-unbound 2.365 and 3.502/3.547 MeV states in ^{13}N. Laboratory α-particle spectra corresponding to these three modes have been generated in Monte Carlo simulations using single-channel, single- and multilevel *R*-matrix formulas. A fit of these spectra to the α spectrum resulting from a triple-coincidence measurement results in excellent agreement with the experimental spectrum and allows branching ratios to be deduced for these rare decay modes.

DOI: 10.1103/PhysRevC.66.064316 PACS number(s): 27.20.+n, 23.50.+z, 23.60.+e, 26.20.+f

I. INTRODUCTION

The β-delayed particle decay of ^{17}Ne into unbound states in ^{16}O offers, in principle, the possibility of determining the reduced α widths of the $J^\pi=1^-$ bound state at $E_x=7.117$ MeV and the $J^\pi=2^+$ bound state at $E_x=6.917$ MeV in ^{16}O. These reduced α widths are intimately related to the strength of the $E1$ and $E2$ components in the astrophysically important ^{12}C$(\alpha,\gamma)^{16}$O radiative capture reaction [1–3]. These components are poorly constrained by present α-capture data and will be difficult to determine by future direct measurements [3].

Some years ago, the β-delayed α-particle spectrum from ^{16}N was used to constrain the $E1$ cross section at low energies by determining the α width of the subthreshold 1^- state, thereby much reducing the uncertainty in the ^{12}C$(\alpha,\gamma)^{16}$O $E1$ cross section at 300 keV [4,5]. However, 2^+ states are not significantly populated in the decay of ^{16}N and our knowledge of the $E2$ component was not improved by that experiment. In the β-delayed proton decay of ^{17}Ne, both 1^- and 2^+ states in ^{16}O are populated. Therefore, the decay of ^{17}Ne has been investigated to see if the strengths of the tails of both the 6.917 and 7.117 MeV subthreshold states in the ^{12}C$(\alpha,\gamma)^{16}$O reaction could be determined [6].

Our study of the decay of ^{17}Ne led to the first observation of β-delayed proton-alpha ($\beta\, p\alpha$) and alpha-proton ($\beta\ \alpha p$) decay of ^{17}Ne through the isobaric analog state (IAS) in ^{17}F [7]. The modes observed were[1]

$$
\begin{aligned}
^{17}\mathrm{Ne} \rightarrow \beta^+ + {}^{17}\mathrm{F}(11.193) & \\
\rightarrow {}^{16}\mathrm{O}(9.585)+p \qquad & \rightarrow {}^{12}\mathrm{C}(0)+\alpha+p \\
\rightarrow {}^{13}\mathrm{N}(2.365)+\alpha \qquad & \rightarrow {}^{12}\mathrm{C}(0)+p+\alpha \\
\rightarrow {}^{13}\mathrm{N}(3.50/3.55)+\alpha & \rightarrow {}^{12}\mathrm{C}(0)+p+\alpha.
\end{aligned}
$$

A partial level scheme showing these three decay modes is shown in Fig. 1. A detailed study of the first decay mode could provide an independent check on the $E1$ strength in ^{12}C$(\alpha,\gamma)^{16}$O.

The energy difference between the IAS in ^{17}F and the threshold for breakup into $\alpha+^{12}$C in ^{16}O is 3.431 MeV [8]. This energy is well defined since the IAS has a width of only 0.18 keV. In the experiment reported in Ref. [7], a narrow peak at this energy was apparent in the triple-sum coincidence spectrum. In addition, several strong background peaks that could not be removed completely by kinematic cuts were observed. Separated proton, α and ^{12}C spectra were obtained with a gate set on the 3.431 MeV triple-sum peak. In these spectra the breakup of the IAS into three particles via the three channels noted above was observed. However, the branching ratios for the three channels were uncertain as the detector arrangement had not been optimized. In

*Present address: Bubble Technology Industries, Chalk River, ON, Canada K0J 1J0.

†Present address: Radiomed, Tyngsboro, MA 01879.

‡Present address: Physikalisch-Technische Bundesanstalt, Braunschweig, Germany.

§Present address: Department of Physics and Astronomy, The University of North Carolina at Chapel Hill, Chapel Hill, NC 27599-3255.

‖Present address: National Superconducting Cyclotron Laboratory, Michigan State University, East Lansing, MI 48824-1321.

¶Present address: TRIUMF, 4004 Wesbrook Mall, Vancouver, BC, Canada V6T 2A3.

[1]The 3.502 and 3.547 MeV states with widths of 62 and 47 keV, respectively, are too close in energy to be separated with the resolution available in this work. Transitions which may take place to one or the other, or both, of these states are labeled by (3.50/3.55) to indicate this uncertainty.

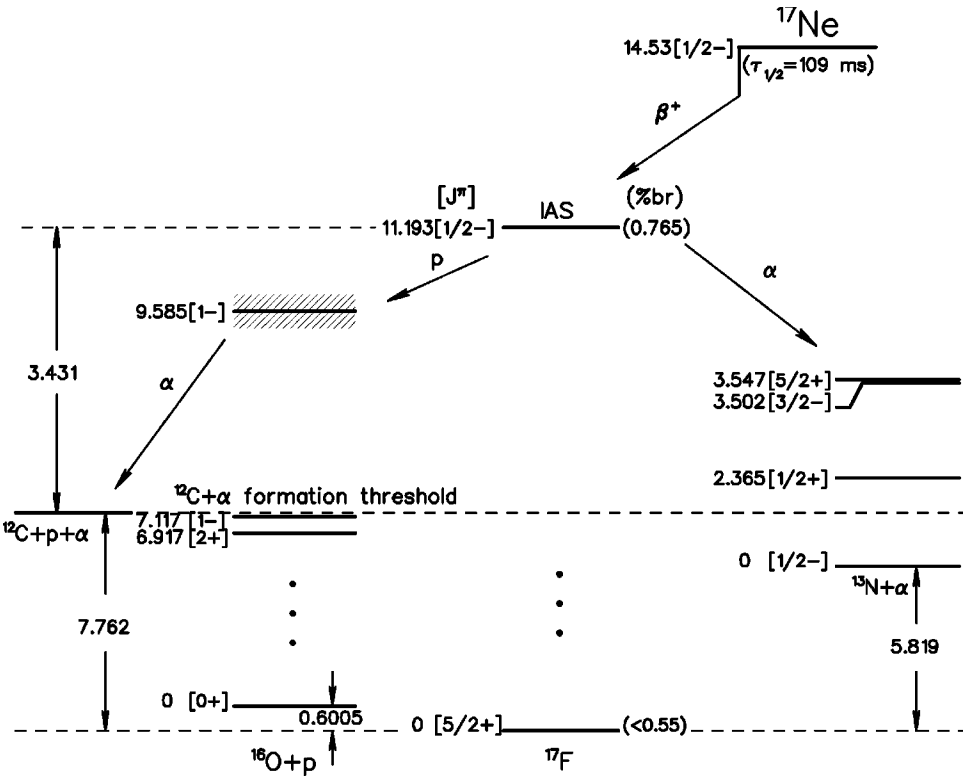

FIG. 1. Partial decay scheme of ^{17}Ne [6,8–11].

this paper we report the results from higher-resolution, lower-background experiments.

II. EXPERIMENT

In Ref. [7] an experimental arrangement consisting of two 900 mm^2 ion-implanted Si detectors (PIPS) at right angles, and two 450 mm^2 PIPS detectors placed at 110^o to one of the larger detectors, was used to study the decay of the IAS via proton-α-^{12}C triple coincidences. The ^{17}Ne beam was obtained from the TISOL facility [12] at TRIUMF. However, the close geometry of this arrangement resulted in spectra contaminated by random-coincidence events which could not be removed by the kinematic cuts applied to the data.

In a second experiment the larger ion-implanted detectors were replaced by two 5 cm$\times$5 cm$\times$300 μm double-sided silicon strip detectors (DSSD's) with 16 strips per side, with adjacent strips connected together to give 64 pixels per detector. The experimental setup (see Fig. 2) consisted of these two DSSD's and two telescopes, each of which consisted of two 900 mm^2 PIPS detectors with thickness of 300 μm and 700 μm. The thicker PIPS detectors were placed behind the thinner ones to veto punch-through particles. A gate was set on the IAS peak in the triple-sum spectrum and the final alpha spectrum, with all possible combinations of particle identities, was generated. These data confirmed the results from the previous experiment [7] where three alpha groups in the three-body breakup of the IAS in ^{17}F were observed. A kinematic procedure was developed (see Sec. III A) that took into account the observed energies and their uncertainties, the positions and sizes of the detector elements, and the angles between pairs of trajectories. The small size of detec-

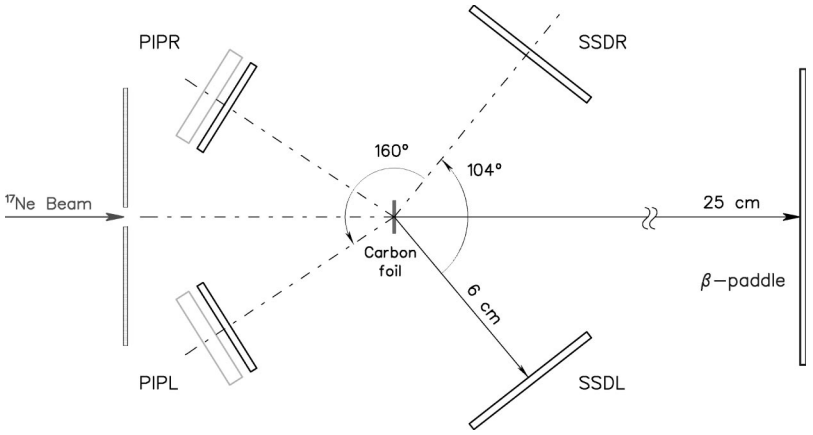

FIG. 2. Setup for the triple-coincidence experiment using double-sided silicon strip detectors (SSDR and SSDL).

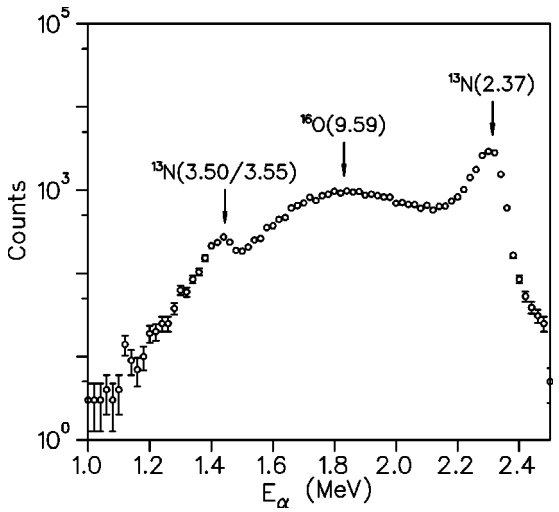

FIG. 3. The final α spectrum from the triple-coincidence experiment. There are 41 732 counts in the spectrum.

tor elements (pixels) inherent to the DSSD also provided tighter constraints compared with those given by the earlier setup in which only large-size PIPS detectors were used. The final alpha spectrum is shown in Fig. 3.

To further improve the resolution and to reduce the random-coincidence background, the breakup of the IAS in ^{17}F was studied with an improved experimental arrangement. The DSSD and PIPS detectors were moved to 10 cm from the collector foil, and scintillator paddles were placed just outside the detector array so that they subtended a solid angle of about 25% of 4π at the collector foil (see Fig. 4). Moving back the detectors reduced the solid angle subtended by each detector element, while the presence of the scintillators meant that a quadruple coincidence (β-p-α-^{12}C) could be obtained with reasonable efficiency.

The results from this run were not as useful as anticipated for two main reasons. The time resolution of 3 ns from the DSSD's was adequate to allow separation of α and proton groups in the DSSD's below an energy of 3 MeV. However,

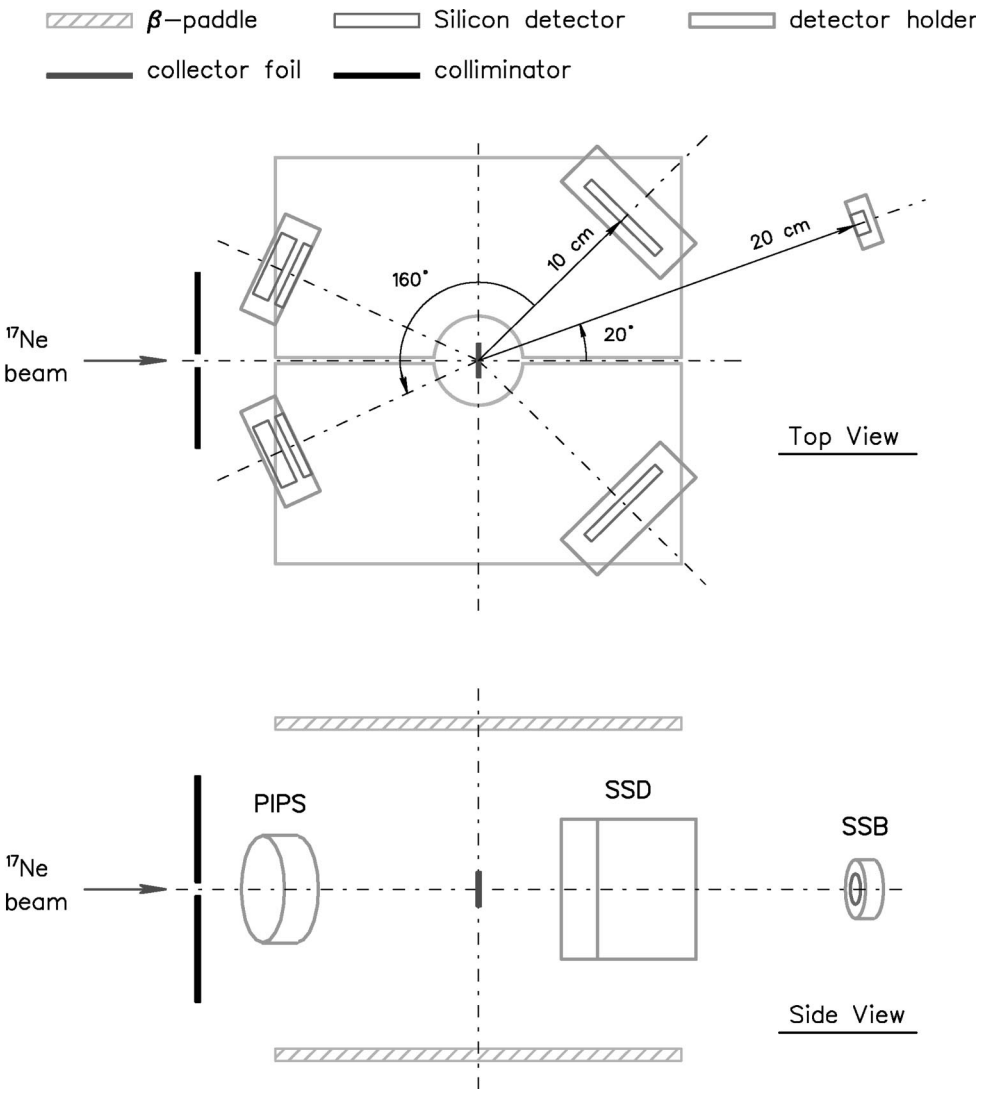

FIG. 4. Experimental setup for quadruple-coincidence measurements. The same silicon detectors from the triple-coincidence run were used. In addition, four scintillator paddles, subtending a solid angle of approximately 25% of 4π, were placed just outside the detector array. The silicon surface barrier detector (SSB) was used to record single-particle spectra [6,13].

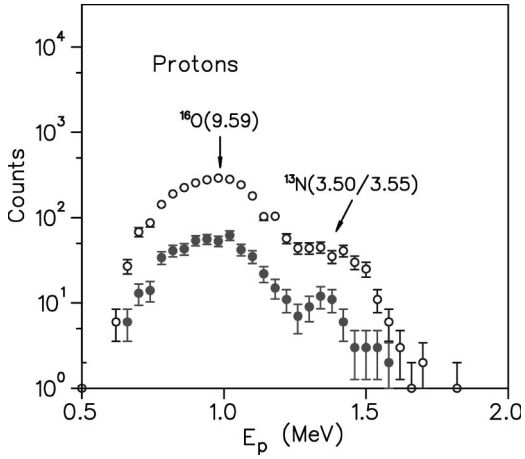

FIG. 5. Final triple- and quadruple-coincidence spectra of protons from the setup of Fig. 4. There are 2829 triple and 557 quadruple coincidences.

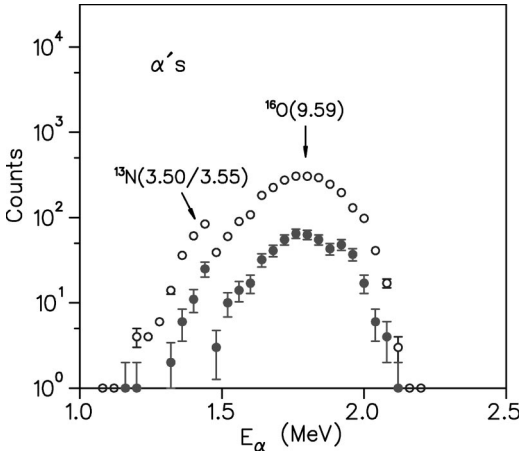

FIG. 6. Final triple- and quadruple-coincidence spectra of α particles from the setup of Fig. 4. There are 2829 triple and 557 quadruple coincidences.

the time resolution with the PIPS detectors of about 15 ns resulted in a much larger background in the coincidence spectra than had been expected. The use of a microchannel or microsphere plate to improve time resolution for recoil nuclei was investigated but ultimately rejected because of the large stable beam current (>1 μA) from TISOL at mass 17, presumably due to $(^{16}\mathrm{OH})^+$. The mass resolution of TISOL was not sufficient to separate the ^{17}Ne beam from this background. In addition, the yield of ^{17}Ne from TISOL, although initially $>10^5$ s^{-1}, decreased steadily during the run to near 10^4 s^{-1}. With the detector solid angle reduced by moving the detectors farther from the collector foil, this relatively low ^{17}Ne beam meant that far fewer triple and quadruple coincidences were obtained than had been expected.

The relatively poor timing resolution and low ^{17}Ne yield meant that, while improved triple-sum and α spectra were obtained, they were neither as pure as expected nor did they contain as many counts as those obtained previously. A much bigger improvement in background level in the triple-sum spectrum resulted from the smaller solid angle subtended by each pixel in the DSSD's than from the implementation of an additional β-coincidence requirement. In the final triple- and quadruple-coincidence proton and α spectra shown in Figs. 5 and 6, the peaks in the spectra due to the IAS$\rightarrow$2.365 transition (very prominent in the α spectrum of Fig. 3) have been completely eliminated, as the reduced pixel solid angle makes the detection of this decay mode kinematically unfavored.

III. DATA ANALYSIS

The α spectrum from the first triple-coincidence experiment with strip detectors was chosen for detailed analysis. The presence of the transition to the 2.365 MeV state in ^{13}N provided a means to obtain absolute branching ratios for the other two transitions, since the branching ratio for this transition is known from analysis of ratio-cut and time-of-flight spectra [6,13].

A. Kinematic procedure

In order to discriminate by kinematic constraints against background, a procedure was developed to process the data on an event-by-event basis [14]. The procedure consists of minimizing a function which depends on the observed energies of the particles, the locations of the detector elements, and the uncertainties of these observables. The magnitude of this function, which is similar to a χ^2, reflects the goodness of an event; this quantity should not be treated strictly as a χ^2 since the distributions of some of the variables are not necessarily normal. Nevertheless, a large value of this function associated with any event can be taken as an indication that the event is kinematically unfavored.

Numerous forms for the kinematic function were tested. The major differences among these functional forms were in the treatment of linear momentum conservation and the choice of physical quantities to be constrained. The final form consists of only six terms grouped into three components,

$$S=\frac{S_1+S_2+S_3}{6}, \tag{1}$$

where

$$S_1=\sum_{i=p,\alpha,c}\frac{(E_i-e_i)^2}{\sigma_{e_i}^2},$$

$$S_2=\frac{(\Theta_{p\alpha}-\theta_{p\alpha})^2}{\sigma_{\theta_{p\alpha}}^2}+\frac{(\Theta_{pc}-\theta_{pc})^2}{\sigma_{\theta_{pc}}^2},$$

and

$$S_3=\frac{\left[\left(\sum_{i=p,\alpha,c}e_i\right)-Q_{3\mathrm{b}}\right]^2}{\sigma_{Q_{3\mathrm{b}}}^2}.$$

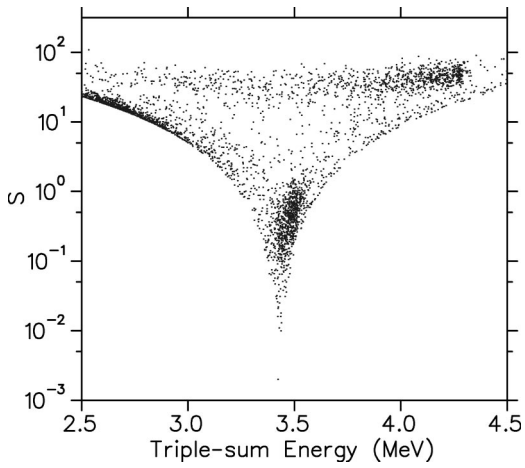

FIG. 7. Result of kinematic procedure: S versus triple-sum energy. The quantity S reflects the goodness of an event.

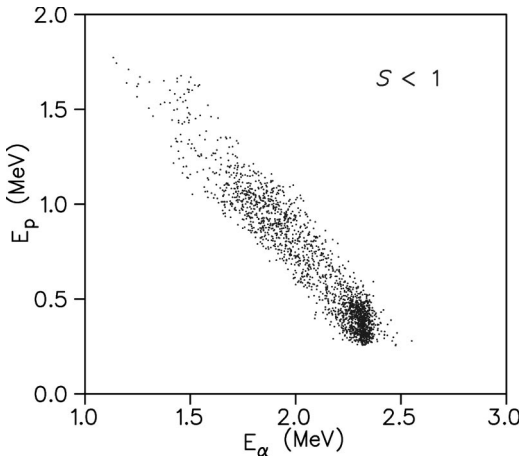

FIG. 9. Energy relation between protons and α particles with an upper limit of unity set on S.

In S_1, e_i are the observed energies with uncertainties σ_{e_i} and E_i are the energies determined from the fit procedure (see below). In S_2, $\theta_{p\alpha}$ (θ_{pc}) is the angle between the centers of the detector elements in which the p-α (p-^{12}C) pair have been observed; $\Theta_{p\alpha}$ (Θ_{pc}) is the angle between the trajectories of the proton and α particle (proton and ^{12}C) calculated from the fitted energies; and $\sigma_{\theta_{p\alpha}}$ ($\sigma_{\theta_{pc}}$) is the uncertainty in $\theta_{p\alpha}$ (θ_{pc}). The angular uncertainties are taken as the differences between the angles subtended by the centers of a pair of detector elements and the maximum angle subtended by the pair. The α-^{12}C angle $\theta_{\alpha c}$ does not provide an additional constraint since the sum of $\theta_{p\alpha}$, θ_{pc}, and $\theta_{\alpha c}$ should add up to 2π. In S_3, e_i are as in S_1, and Q_{3b} is the three-body breakup Q value. On an event-by-event basis, the CERN package MINUIT [15] was used to obtain the minimum of S, which is returned as the average of the six terms. In a strict sense, only the three energies are variables in the minimization, while the other three quantities are calculated from the fitted energies; conservation of momentum is implicit in the calculation of $\theta_{p\alpha}$ and θ_{pc} from the fitted energies. The inclusion of the three-body breakup Q value as a constraint is very effective in distinguishing events from a given parent state in ^{17}F.

The function S was calculated for each event in the final reduced data set. From the result shown in Fig. 7, it is clear that the value of S for most events near the three-body breakup Q value of the IAS (3.431 MeV) is less than unity. It is also clear that there is a separation between these events and the bands of suspected false events at higher S, which extend across a much larger range of energies. The separation between these events and those on either side of the minimum is also distinct. Accordingly, we set an upper limit of unity on S as a criterion for extraction of kinematically valid events. The energy relation between protons and α particles before setting a limit on S is shown in Fig. 8. The result of imposing an upper limit of unity on S, along with moderate timing constraints, is shown in Fig. 9. The α spectrum projected from Fig. 9 is that shown in Fig. 3.

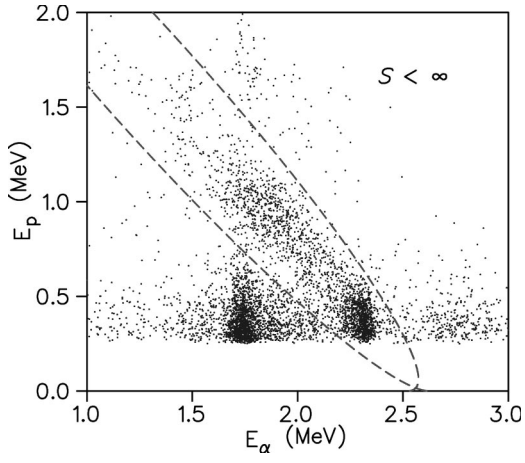

FIG. 8. Energy relation between protons and α particles with no upper limit set on S. The dashed lines indicate the region in which events satisfying both momentum and energy conservation for decay from the IAS must lie.

B. *R*-matrix formalism

Assuming that the breakup takes place in a two-step sequential process, that the parent state in ^{17}F is identified (i.e., the three-body breakup Q value is known), and that the angle between the two emitted radiations (p and α) is determined, then the kinematics of the three-body breakup of an excited state in ^{17}F into a final state of $p+\alpha+{}^{12}$C are completely determined once the energy of the intermediate state in ^{16}O or ^{13}N is known. We first assume that only a single level in the intermediate state contributes to the decay. Therefore, for the case of ^{16}O (^{13}N) the entrance channel is ^{17}F(IAS) $\rightarrow {}^{16}$O(9.585)$+p$ [^{17}F(IAS)$\rightarrow {}^{13}$N (2.365 or 3.50/3.55)$+\alpha$] and the exit channel is ^{16}O(9.585)$\rightarrow {}^{12}$C$+\alpha$ [^{13}N(2.365 or 3.50/3.55)$\rightarrow {}^{12}$C$+p$]. The appropriate R-matrix equation to describe the ^{16}O state[2] is [14]

[2]Spectra for decays through the ^{13}N channel can be obtained similarly by switching the roles of the proton and α particle.

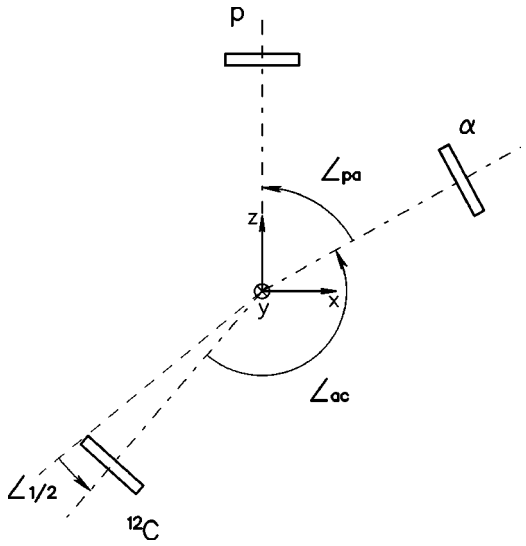

FIG. 10. A typical system of three detectors for the measurement of triple coincidences.

$$N_\lambda(E)=A^2P_p\left|\frac{\dfrac{C_\lambda\gamma_\lambda}{E_\lambda-E}}{1-(S_\alpha-b_\alpha+iP_\alpha)\dfrac{\gamma_\lambda^2}{E_\lambda-E}}\right|^2 P_\alpha, \quad (2)$$

where A^2 is a normalization constant that is a function of the number of counts in a spectrum; P_p and P_α are the proton and α penetration factors, respectively; γ_λ^2 is the reduced width belonging to the state λ, where λ labels the intermediate state; C_λ is a proton-feeding parameter to the state of energy E_λ; S_α is the shift function; and b_α is the boundary constant.

If there is only one feeding channel, this can be extended to the multilevel case by summing over the levels; i.e.,

$$N(E)=A^2P_p\left|\frac{\displaystyle\sum_\lambda\frac{C_\lambda\gamma_\lambda}{E_\lambda-E}}{1-(S_\alpha-b_\alpha+iP_\alpha)\displaystyle\sum_\lambda\frac{\gamma_\lambda^2}{E_\lambda-E}}\right|^2 P_\alpha. \quad (3)$$

C. Calculations of laboratory spectra

Equations (2) or (3) cannot be used directly to fit the experimental spectra since the present case involves three-body kinematics and the observed particle spectra depend on the geometry of the detection system. A typical detection system for the observation of three-body breakups is depicted in Fig. 10. The three parameters that completely specify the system are $\angle_{pa}$, the angle between the proton and α detectors; $\angle_{ac}$, the angle between the α and carbon detectors; and $\angle_{1/2}$, the half angle[3] subtended by a detector.

TABLE I. Variables used in the *R*-matrix calculation of laboratory particle spectra.

Variable	Description
Q	three-body breakup Q value (=3.431 MeV for decays from the IAS in ^{17}F)
θ_p	angle between the center of a pixel in the proton detector and the z axis
E	excitation energy of the intermediate state (^{16}O or ^{13}N)
θ'	angle between the two emitted radiations p and α
E_p, E_α, E_c	laboratory particle energies
ϕ	azimuthal angle of decay plane
N	contribution to energy spectrum calculated from Eq. (2) or Eq. (3)
Ω_p	solid angle subtended by a pixel in the proton detector

The detection system of Fig. 2 contains two combinations of three detectors, and particle spectra were obtained by summing contributions from the two combinations as they have the same geometry.

The variables used in the calculations of laboratory particle spectra for a definite detection geometry, and through a definite decay channel, are listed in Table I. For the case of the ^{16}O channel we first assume the proton detector to be a point detector on the $+z$ axis, and place the α and carbon detectors on the xz plane with their active surfaces towards the origin and with the polar angles of their centers determined by $\angle_{pa}$ and $\angle_{ac}$. We further assume that the decay takes place on the xz plane with the decay vertex located at the origin. With the direction of the proton fixed, observation of a three-body breakup requires the trajectories of both the α particle and the carbon ion to strike their respective detectors. The kinematics are completely determined once E, θ', and the three-body breakup Q value are determined. Equations relevant to the calculation of laboratory energies and directions of the particles using the above variables are given in Ref. [14]. If the calculated paths of the α particle and carbon ion intersect their respective detectors, the energy bins of values E_p, E_α, and E_c of the respective particle spectra are incremented by an amount N obtained with Eq. (2). Full-energy spectra can then be obtained by integrating E over the range determined by the three-body breakup Q value, θ' over the range $[0,\pi]$, and ϕ over the range subtended by the α and carbon detectors to account for their finite size (i.e., the breakup does not necessarily take place on the xz plane).

Up to this point, the proton detectors have been treated as point detectors. In order to account for their finite size, the detectors are divided into $n\times n$ pixels where n is the number of readouts per side of a DSSD.[4] Each pixel in a proton detector can then be treated as a point detector as before.

[3]To a good approximation, the half angle is proportional to the radius for a circular detector and is proportional to half the length of an edge for a square detector.

[4]n also reflects the angular resolution of the system, which in turn affects the accuracy of the calculation.

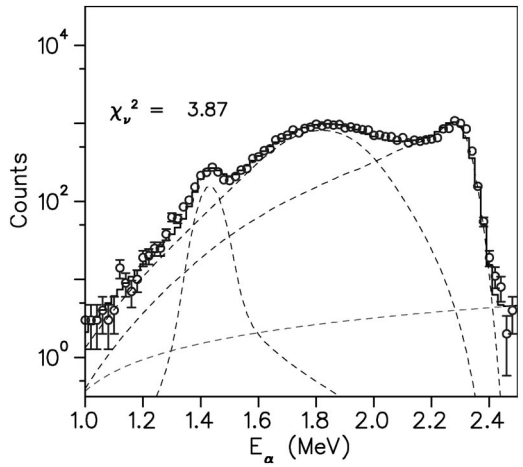

FIG. 11. Final alpha spectrum from the triple-coincidence experiment obtained with an upper limit of unity on *S*. The solid line is the calculated fit using a single-channel, single-level *R*-matrix formula for each transition; the dashed lines are the calculated contributions for each channel.

Details of the calculations required to account for the finite size of the detectors (and of the finite size of the target spot on the collector foil) can be found in Ref. [14]. These kinematic and experimental considerations were used, along with Eq. (2) or Eq. (3), in a Monte Carlo algorithm [14] to generate the α spectra for the three decay channels which were then fitted, along with a very small background term, to the experimental α spectrum as shown in Fig. 11. The fit resulted in the branching ratios (BR's) of $7.9\pm2.2\%$ for the IAS$\rightarrow$9.585 transition (BR_1) and $0.9\pm0.5\%$ for the IAS $\rightarrow$3.50/3.55 transition (BR_2) relative to the BR for the proton transition from the IAS to the 7.117 MeV state in ^{16}O. The BR of $37.5\pm2.8\%$ from Ref. [6] for the IAS$\rightarrow$2.365 transition was used to normalize the present BR's to those of Ref. [6]. These branching ratios have been included in the complete set of branching ratios for the decay of ^{17}Ne listed in Ref. [6].

1. Error analysis

Two sources contribute to the statistical error: the uncertainty in the relative BR's to the 2.365 and 7.117 MeV states; and the statistical uncertainty in fitting the spectrum. The calculation of the first source of error is straightforward and results in contributions of 0.75% and 0.08(5)% to BR_1 and BR_2, respectively. The error due to the fitting procedure can be obtained from the covariance matrix calculated by MINUIT [15] at the 1σ level. Caution has been taken, by using different minimization algorithms provided by MINUIT and by varying the initial values, to ensure that the absolute minimum has been found. Based on results of the best fit, we obtain contributions to the error due to the fit of 0.96% and 0.4(1)%, respectively. Since the two sources of error are independent, they can be added in quadrature resulting in total statistical errors of 1.2(3)% for BR_1 and 0.4(2)% for BR_2.

At least three types of uncertainties contribute to the systematic error: those due to the kinematic procedure in extracting the final experimental spectrum; that in the proton energy threshold; and those in geometric detection efficiency due to uncertainties in locations of detectors and the finite size of the beam spot. The error associated with the kinematic procedure was estimated by fitting the calculated spectrum to the experimental spectrum while varying the upper limit on the kinematic parameter by 20% about $S=1$, i.e., from 0.8 to 1.2. Based on these fits, BR_1 and BR_2 were then calculated and compared with the values obtained with $S \leqslant 1$. The results show a variation of 0.65% in BR_1 and 1.45% in BR_2, giving contributions of 0.05(2)% and 0.02(3)%, respectively, to the systematic errors. This shows that the relative BR's are not very sensitive to the upper limit of the kinematic parameter.

In order to estimate the errors due to the uncertainty in proton energy threshold, the experimental spectrum was fitted with calculated spectra whose proton threshold varied by ±10 keV about the best-fit value of 500 keV, corresponding to a spread in χ^2 of about 20%. This produced a variation in BR_1 of 16.2% and in BR_2 of 12.3%, giving contributions to the error of 1.2(9)% and 0.11%, respectively.

The uncertainties in geometric detection efficiency are due to two factors: the uncertainty in the locations of the detector elements, which is about 2^o; and the effect of the finite size of the beam spot. In order to estimate the error due to location uncertainty, detection efficiencies were calculated with the detectors moved in turn by 2^o. This new set of efficiencies was then compared with that obtained with the detectors at the original positions, and the largest deviations were taken as errors. This calculation results in errors in detection efficiency of 2.5%, 15.9%, and 12.3% for the 9.585, 2.365, and 3.50/3.55 channels, respectively. It is apparent that the efficiency of the 9.585 channel is much less sensitive to the locations of the detectors than is the efficiency of the other two channels. This is because the system was designed so that the angle between the proton and α detectors is 160^o, the most probable (laboratory) angle between the proton and α particle for decays from the 9.585 channel; the corresponding angle for the 2.365 channel is 167^o while that for the 3.50/3.55 channel is 148^o [14].

From an inspection of the collector foil at the end of the experiment, the beam spot was determined as roughly circular with a diameter of about 8 mm. However, an analytical calculation of the error in efficiency due to a finite beam spot is difficult since the actual distribution of the ions within the beam spot is not known, and the calculation involves a transformation and rotation of coordinate systems which is tedious to handle analytically. Instead, a Monte Carlo simulation was performed to study this effect assuming the ions were distributed normally within the beam spot. The results from the Monte Carlo study show that, compared with results obtained with a pointlike beam spot, the efficiency is altered by 2.6%, 1.7%, and 3.1%, respectively, for the 9.585, 2.365, and 3.50/3.55 channels. These errors are then added in quadrature to those obtained from the consideration of the uncertainties in the locations of the detectors. The results are 3.6%, 16.0%, and 12.7% for the three channels, respectively. With these uncertainties in detection efficiency, we find contributions of 1.3(0)% and 0.18(4)% for BR_1 and BR_2, re-

TABLE II. Branching ratios for the decay of the IAS in ^{17}F expressed as a percentage of the total IAS decay strength.

Emitted particle	Final state		Branching ratio Ref. [16]	Ref. [17]	Present
p	^{16}O	9.585			1.9±0.5 [a]
		8.872			15.7±2.6 [b]
		7.117	44±4	18±3	23.8±1.3 [b]
		6.917	24±6	<4	0.56±0.19 [b]
		6.130	22±2	25±2	31.9±1.3 [b]
		6.049	<3	11±3	5.8±0.4 [b]
		0	9.3±1.3	10.7±0.6	8.2±0.5 [b]
α	^{13}N	3.502/3.547			0.2±0.1 [a]
		2.365	<7	29±9	8.9±0.7 [b]
		0		1.1±0.5	0.3±0.1 [b]
γ	^{17}F	0.495		3.4±1.5	2.8±1.3 [c]

[a]From triple-coincidence experiment.
[b]From Ref. [6].
[c]Calculated from Refs. [17–19], taking into account previously unobserved transitions.

spectively. Since the three sources of systematic error are independent of one another, they can be added in quadrature to obtain the final total systematic error of 1.8(3)% for BR_1 and 0.2(2)% for BR_2.

As a result of this error analysis, we find $BR_1 = 7.9 \pm 1.2 \pm 1.8\%$ and $BR_2 = 0.9 \pm 0.4 \pm 0.2\%$, where the statistical error is given first. Assuming the statistical and systematic errors to be independent, they can be combined to give $BR_1 = 7.9 \pm 2.2\%$ and $BR_2 = 0.9 \pm 0.5\%$, as quoted above.

2. Comparison with previous work

The present branching ratios supercede those given in Table I of Ref. [7]. They are included in the complete set of branching ratios for the decay of the IAS given in Table 7 of Ref. [6]; this table is reproduced here (Table II) for ease of reference. The branching ratios for $\beta\, p\alpha$ and $\beta\, \alpha p$ decay of the IAS differ from those of Ref. [7] for two reasons. First, the branching ratio for the α decay to the 2.365 MeV state, which is used to normalize the two-particle decay modes to the single-particle decays, has changed due to the discovery of additional decay modes as explained in Ref. [6]. Second, the present experimental setup is better understood than that used in Ref. [7] and the *R*-matrix analysis provides a firmer basis for the calculation of the branching ratios and the assignment of errors.

IV. SUMMARY AND CONCLUSIONS

The isobaric analog state in ^{17}F has been observed to break up into a proton, an α particle, and a ^{12}C nucleus via three channels: through the 9.585 MeV state in ^{16}O; and through the 2.365 and the 3.502 and/or 3.547 MeV state(s) in ^{13}N. The branching ratio for the α decay of the IAS to the 2.365 MeV state has been measured via particle-decay studies [6] to be 37.5±2.8 relative to the proton decay branching ratio from the IAS to the 7.117 MeV state in ^{16}O, which was set at 100. A fit to the α spectrum resulting from the breakup of the IAS, which included the channel through the 2.365 MeV state, resulted in a relative branching ratio of 7.9±2.2 for proton decay to the 9.585 MeV state in ^{16}O, and 0.9 ±0.5 for α decay to the 3.50/3.55 MeV state(s) in ^{13}N. Only sequential $p\alpha$ and αp decays were assumed in the formulation of the *R*-matrix expressions used to generate the fit to the experimental spectrum; the goodness of the fit to the spectrum justifies this assumption.

The discovery of proton decay from the IAS to the 1^- states in ^{16}O at 7.117 and 9.585 MeV suggested the possibility of observing interference between the 9.585 MeV state and the tail of the 7.117 MeV state in a triple-coincidence α spectrum. This could result in a determination of the α width of the 7.117 MeV state and give an independent estimate of $S(E1)$ for the astrophysically important $^{12}\mathrm{C}(\alpha,\gamma)^{16}\mathrm{O}$ reaction. The conditions required to optimize a set of detectors to produce such a spectrum have been investigated sytematically using an *R*-matrix Monte Carlo approach [14]. The spectrum resulting from these calculations suggests that interference could be observed in such a spectrum if sufficient ^{17}Ne beam were available for the observation of $\approx 1 \times 10^6$ triple coincidences in an optimized multidetector system.

ACKNOWLEDGMENTS

We wish to thank H. Biegenzein, D. Jones, P. Machule, and H. Sprenger for helping with the technical aspects of this experiment and M. Trinczek for assistance with the data collection. We thank E. Vogt for valuable discussions concerning the treatment of three-body breakup in *R*-matrix theory. R.E. Azuma provided valuable comments at all stages of this work. The work was supported in part by the Natural Sciences and Engineering Research Council of Canada, the National Science Foundation (Grant No. PHY9901241), the United Kingdom Science and Engineering Research Council, and by TRIUMF.

[1] W.A. Fowler, Rev. Mod. Phys. **56**, 149 (1984).
[2] T.A. Weaver and S.E. Woosley, Phys. Rep. **227**, 65 (1993).
[3] L. Buchmann, R.E. Azuma, C.A. Barnes, J. Humblet, and K. Langanke, Phys. Rev. C **54**, 393 (1996).
[4] L. Buchmann *et al.*, Phys. Rev. Lett. **70**, 726 (1993).
[5] R.E. Azuma *et al.*, Phys. Rev. C **50**, 1194 (1994).
[6] A.C. Morton *et al.*, Nucl. Phys. **A706**, 15 (2002).
[7] J.C. Chow *et al.*, Phys. Rev. C **57**, R475 (1998).
[8] D.R. Tilley, H.R. Weller, and C.M. Ceves, Nucl. Phys. **A564**, 1 (1993).
[9] J.D. King *et al.*, in *Proceedings of the Fourth International Symposium on Nuclear Astrophysics: Nuclei in the Cosmos, Notre Dame, 1996*, edited by J. Görres, G. Mathews, S. Shore, and M. Wiescher [Nucl. Phys. **A621**, 169c (1997)].

[10] J.D. King *et al.*, in *Proceedings of the International Workshop on the Physics of Unstable Nuclear Beams, Serra Negra, São Paulo, Brazil, 1996*, edited by C.A. Bertulani, L. Felipe Canto, and M. S. Hussein (World Scientific, New Jersey, 1997), p. 15.
[11] J.D. King *et al.*, in *Tours Symposium on Nuclear Physics III*, edited by M. Arnould, M. Lewitowicz, Yu.Ts. Oganessian, M. Ohta, H. Utsonomiya, and T. Wada, AIP Conf. Proc. No. 425 (AIP, Woodbury, New York, 1998), p. 372.
[12] J.M. D'Auria, L. Buchmann, M. Dombsky, P. McNeely, G. Roy, H. Sprenger, and J. Vincent, Nucl. Instrum. Methods Phys. Res. B **70**, 75 (1992).
[13] A.C. Morton, Ph.D. thesis, University of Toronto, 2001.
[14] J.C. Chow, Ph.D. thesis, University of Toronto, 2001.
[15] F. James, *MINUIT Function Minimization and Error Analysis Reference Manual and Version 94.1*, CERN Program Library entry D506, Geneva, 1994.
[16] J.C. Hardy, J.E. Esterl, R.G. Sexto, and J. Cerny, Phys. Rev. C **3**, 700 (1971).
[17] M.J.G. Borge *et al.*, Nucl. Phys. **A490**, 287 (1988).
[18] M.N. Harakeh, P. Paul, and K.A. Snover, Phys. Rev. C **11**, 998 (1975).
[19] F. Hinterberger, P. von Rossen, B. Schüller, J. Bisping, and R. Jahn, Nucl. Phys. **A263**, 460 (1976).